Model-based trajectory planning for flexible-link mechanisms with bounded jerk

P. Boscariol, A. Gasparetto
DIEGM, University of Udine
Via delle Scienze 206, 33100, Udine, Italy

Abstract

This paper deals with the model-based development of optimal jerk-limited point-to-point trajectories for flexible-link robotic manipulators. In the proposed approach, an open-loop optimal control strategy is applied to an accurate dynamic model of flexible multi-body planar mechanisms. The model, which has already been fully validated through experimental tests, is based on finite element discretization and accounts for the main geometric and inertial nolinearities of the linkage. Exploiting an indirect variational solution method, the necessary optimality conditions deriving from the Pontryagin's minimum principle are imposed, and lead to a differential Two-Point Boundary Value Problem (TPBVP); numerical solution of the latter is accomplished by means of collocation techniques. The resulting motion and control profiles can be used as feedforward reference signals for a position and vibration control. Considering a lightweight RR robot, simulation results are provided for rest-to-rest, jerk-limited trajectories with minimum actuator jerks and vibrations. However, the strategy under investigation has general validity and can be applied to other types of mechanisms, as well as with different objective functions and boundary conditions. Numerical evidence clearly indicates that the use of a composite cost functional and the imposition of jerk constraints can greatly reduce vibration phenomena during high-speed motion of flexible-link manipulators.

1 Introduction

High speed operation is a recurring target in design and application of robotic manipulators, for clear economic reasons. Also maximizing the ratio between the weight of the payload and that of the whole mechanism is a common objective. Traditionally, to ensure a good position accuracy of manipulators, their arms have been designed and built so as to behave like rigid bodies. Hence, conventional robots still present heavy links and bulky structures. However, such systems are shown to be inefficient in terms of actuator power consumption and speed, related to their load-carrying capacity [1], as payload-to-manipulator weight ratio is typically ranging from 1:100 to 1:10 [2].

On the other hand, a common trend of robot design is to develop lightweight mechanisms also for industrial applications, not only for weight-critical tasks such as outer space explorations. Lighter robots exhibit several advantages over heavy rigid ones, such as lower cost, improved energy efficiency and safety, higher operating speed and payload-to arm weight ratio. Despite this, lower arm stiffness generates flexibility and vibration issues. In these cases, dynamic analysis and control strategies based on the rigid-link assumption turn out to be no longer

P. Boscariol, A. Gasparetto
Model-based trajectory planning for flexible-link mechanisms with bounded jerk
Robotics and Computer Integrated Manufacturing 29(4), pp.90-99, 2013

adequate: structural flexibility, if neglected or poorly controlled, can lead to major worsening in the accuracy of positioning and motion, to high mechanical stress, and also to instability.

During the last 30 years, large efforts have been made in both academic and industrial settings, to offer solutions to the aforementioned problems. Several approaches have been explored, focusing on the main tasks of dynamic modeling, control and trajectory planning of Flexible-Link Manipulators (FLM) [1].

FLMs are continuous nonlinear dynamical systems, possessing an infinite number of elastic degrees of freedom. A crucial aspect is thus represented by the strategy adopted to obtain a finite-dimensional approximation of their dynamics. The main existing approaches are Assumed Mode Method (AMM) and Finite Element Method (FEM), commonly used in combination with the Lagrangian or the recursive Newton-Euler formulations for deriving the system equations of motion. Lumped Parameter modeling, i.e. approximation by means of spring-mass systems, is rarely chosen [3] due to its limited accuracy. If linearized models around a specified operating point are taken into consideration, as done in [4], the dynamics of multi-link FLM is described with limited accuracy: as proved experimentally by Milford and Asokanthan in [5], the eigenfrequencies of a two-link flexible robot can vary up to 30% as a function of the manipulator configuration. Moreover, numerical and experimental studies [6, 7] have demonstrated that an accurate dynamic modeling of FLMs must consider both the coupling between rigid-body and elastic motions and the main geometric and inertial nonlinearities. In Assumed-Mode Method, only a set of eigenfrequencies are used to describe the flexible behaviour of the manipulators, along their whole operative range [3, 8, 9]. FEM formulation is reputed to be more accurate than the AMM in describing flexible multi-link manipulator dynamics, and arms with complex cross-sectional geometries too, as reported by Theodore and Ghosal in [3]. In addition, Lee showed in [10] that conventional Lagrangian modeling of FLMs is not very accurate, in case of rotational motion of the links.

This work concerns the developement of point-to-point optimal path planning algorithms, for planar mechanisms with flexible arms. An highly accurate nonlinear dynamic model of FLMs, based on finite element discretization and Equivalent Rigid-Link System (ERLS) formulation, is used. Global differential equations of motion are obtained by direct application of the principle of virtual work, and they account for the mutual inertial influence between elastic and rigid-body motion [11].

In point-to-point trajectory optimization problems, only the initial and final end-effector positions are given, and the manipulator is free to move between them. The path is therefore subject to optimization, and it is selected with the aim of minimizing a cost functional. Such cost may depend on execution time, actuator effort, jerks (or torque rates), or a combination of these variables. Minimizing actuator jerks, or keeping them bounded, can produce several advantages, such as the reduction of stress induced on actuators and on mechanical structures, and limited excitation of resonance frequencies. Moreover, a very coordinated and natural motion is yielded [12].

The topic of model-based optimal trajectory planning of flexible-link mechanisms is somehow limited, while a large number of strategies has been developed for rigid manipulators [13, 14], also considering the jerk-optimal case [15, 16, 17]. Furthermore, several authors have studied optimal trajectories for robots with mobile bases [18] and/or with flexible joints [19, 20], just to cite a few examples. An interesting approach is also the development of non-time based control strategies, that act as a reference filter, as proposed and tested in [21, 22].

P. Boscariol, A. Gasparetto
Model-based trajectory planning for flexible-link mechanisms with bounded jerk
Robotics and Computer Integrated Manufacturing 29(4), pp.90-99, 2013

As for the optimal control of flexible-link mechanisms, the feedforward techniques used in this paper do not require any additional sensors. They are thus more economical then closed-loop strategies, for vibration control of robotic manipulators performing repetitive tasks [23]. Moreover, their off-line nature allows overcoming many difficulties, such as highly nonlinear dynamics, and system or actuation constraints. The approaches for solving open-loop optimal control problems can be broadly classified into two main categories: direct and indirect methods.

In direct methods, the original optimal control problem is converted into a parameter optimization one [24], by discretizing robot dynamic variables (states and/or controls). Then, an efficient deterministic or stochastic optimization algorithm can be applied to solve this new finite-dimensional problem. In [25] and [26], residual vibration reduction is attained approximating the joint motion profiles with splines or polynomial functions, respectively for a two-link rigid-flexible manipulator and a flexible-link, flexible-joint one. A similar approach is proposed in [27], in which optimal rest-to-rest motion for a two-flexible-link robot is evaluated, using genetic algoritms and polynomial functions. As in most direct approaches to model-based trajectory optimization, dynamic modeling is obtained through the Assumed-Mode Method. An exception is represented by [28]: Finite Element Method is applied to a flexible RR manipulator, in combination with a Genetic Algorithm–fuzzy logic feedback control strategy. Also in [2, 29], a FEM-based modeling for a two-link flexible manipulator is employed: but in this case, an open-loop discrete dynamic programming (DDP) path-planning scheme is proposed. Numerical simulation are perfomed for minimum effort, minimum effort with bounds, minimum time, and minimum torque-rate trajectories. However, Dynamic Programming severely suffers from Bellman's curse of dimensionality [30] and is therefore restricted to systems with low-dimensional state spaces. Moreover, as a result of the control parametrization introduced, all direct methods can only yield approximate solutions to the optimal control problem. Due to the large number of parameters involved, they are extremely time-consuming and quite inefficient, especially for systems with a large number of elastic d.o.f. [31].

On the other hand, indirect methods make use of calculus of variation: necessary conditions for optimality deriving from the Pontryagin's Minimum Principle (PMP) are imposed, and the resulting Two-Point Boundary Value Problem (TPBVP) is solved, by suitable numerical techniques. Indirect methods are widely reckoned to be very accurate, particularly when a large number of elastic d.o.f. is present, or optimization of composite objectives is targeted [32]. In [31], Korayem et al. have developed an algorithm for the point-to-point motion planning of a two-link FLM with revolute joints. Euler-Lagrange formulation and Assumed-Mode Method are used to describe the dynamics of the robot. The cases of minimum effort, minimum effort-speed, maximum payload and minimum vibration are examined; only constraints on joint actuator torques are imposed.

To the best of the authors' knowledge, the only paper applying both FEM-based dynamic modeling and indirect solution methods to the open-loop optimal control problem of FLMs is [33], again by Korayem et al. In it, however, Lagrangian formulation is used to define the robot dynamics, and results are provided only for time evolution of joint speeds and motor torques. Therefore, no results in terms of vibration are presented. Moreover, only minimum effort-speed trajectories are investigated.

In this paper an indirect strategy is developed for the optimal path planning of flexible multi-link manipulators. They minimization of two different objective functions – namely, the time integral of the squared actuator jerks, and a

P. Boscariol, A. Gasparetto
Model-based trajectory planning for flexible-link mechanisms with bounded jerk
Robotics and Computer Integrated Manufacturing 29(4), pp.90-99, 2013

composite cost functional – is considered.

Constraints on control actions – i.e., actuator jerks – are introduced as well, and it will be shown that this feature can further reduce the level of vibration observed during the robot motion. Although only rest-to-rest tasks have been taken into consideration here, the strategy presented here can also be adapted to the most general case of nonzero intial and final conditions, and even to multiple-waypoint trajectory planning. The latter case would require the use of Multi-Point Boundary Value Problem, instead of just a Two-Point BVP.

2 Dynamic modelling

In this section a brief explanation of the dynamic model used for the definition of the trajectory planning problem is given. Such formulation, introduced by Giovagnoni in [11], is based on FEM discretization and on the principle of virtual works. The resulting model, whose high accuracy has been proved in several papers [34, 35, 36], accounts for the inertial non-linearities of the mechanisms and gives a coupled description of both the rigid and flexible motion of a planar FLM with an arbitrary number of links.

First, each flexible link belonging to the mechanism is divided into finite elements. Referring to Figure 1 the following vectors, calculated in the global reference frame $\{X, Y, Z\}$, can be defined:

- $\mathbf{r}_i$ and $\mathbf{u}_i$ are the vectors of nodal position and nodal displacement of the ith element of the ERLS
- $\mathbf{p}_i$ is the position of a generic point inside the ith element
- $\mathbf{q}$ is the vector of generalized coordinates of the Equvalent Rigid-Link System (ERLS)

The vector of positions $\mathbf{b}_i$ is linked to $\mathbf{r}_i$ and $\mathbf{u}_i$ trough:

$$\mathbf{b}_i = \mathbf{r}_i + \mathbf{u}_i \tag{1}$$

since the motion of the nodes of each elastic element is evaluated as the superimposition of the rigid and of the elastic motion. In the same way, also the following vectors can be defined:

- $\mathbf{w}_i$ is the vector that measures the position of a generic point belonging to the ERLS
- $\mathbf{v}_i$ is the vector of the displacement of the point to which $\mathbf{w}_i$ refers, measured from the ERLS
- $\mathbf{p}_i$ is the vector obtained as:

$$\mathbf{p}_i = \mathbf{w}_i + \mathbf{v}_i \tag{2}$$

x_i and y_i are the vectors that define the local reference frame which rotates with the i-th element of the ERLS. ERLS formulation, which has been introduced in [37], is used here to give a fully coupled description of the dynamics of the global coordinates vector $\mathbf{q}$ and of the vector of nodal displacements $\mathbf{u}$. The vectors defined so far are calculated in the global reference frame $\{X, Y, Z\}$. Applying the principle of virtual work:

P. Boscariol, A. Gasparetto
Model-based trajectory planning for flexible-link mechanisms with bounded jerk
Robotics and Computer Integrated Manufacturing 29(4), pp.90-99, 2013

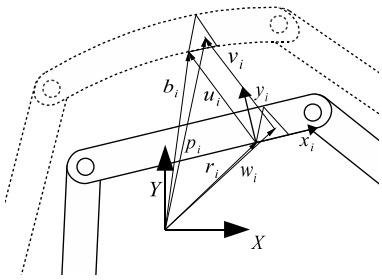

Figure 1: Kinematic definitions of the ERLS

$$\delta W^{elastic} + \delta W^{inertial} + \delta W^{external} = 0 \tag{3}$$

the following relation can be stated:

$$\sum_i \int_{V_i} \delta \mathbf{p}_i{}^T \ddot{\mathbf{p}}_i \rho_i dw + \sum_i \int_{V_i} \delta \epsilon_i{}^T \mathbf{D}_i \epsilon_i dw = \sum_i \int_{V_i} \delta \mathbf{p}_i{}^T \mathbf{g} \rho dw + (\delta \mathbf{u}^T + \delta \mathbf{r}^T)\mathbf{F} \tag{4}$$

where ϵ_i, $\mathbf{D}_i$, ρ_i and $\delta\epsilon_i$ are, respectively, the strain vector, the stress-strain matrix, the mass density of the ith link and the virtual strains. $\mathbf{F}$ is the vector of the external forces, including gravity, whose acceleration vector is $\mathbf{g}$. Eq. (4) shows the virtual works of, respecitvely, inertia, elastic an external forces. From this equation, $\mathbf{p}_i$ and $\ddot{\mathbf{p}}_i$ for a generic point in the ith element are:

$$\begin{aligned} \delta \mathbf{p}_i &= \mathbf{R}_i \mathbf{N}_i \mathbf{T}_i \delta \mathbf{r}_i \\ \ddot{\mathbf{p}}_i &= \mathbf{R}_i \mathbf{N}_i \mathbf{T}_i + 2(\dot{\mathbf{R}}_i \mathbf{N}_i \mathbf{T}_i + \mathbf{R}_i \mathbf{N}_i \dot{\mathbf{T}}_i)\dot{\mathbf{u}}_i \end{aligned} \tag{5}$$

where $\mathbf{T}_i$ is a matrix that describes the transformation from global-to-local reference frame of the ith element, $\mathbf{R}_i$ is the local-to-global rotation matrix and $\mathbf{N}_i$ is the shape function matrix. Taking $\mathbf{B}_i(x_i, y_i, z_i)$ as the strain-displacement matrix, the following relation holds:

$$\begin{aligned} \epsilon_i &= \mathbf{B}_i \mathbf{T}_i \delta \mathbf{u}_i \\ \delta \epsilon_i &= \mathbf{B}_i \delta \mathbf{T}_i \mathbf{u}_i + \mathbf{B}_i \mathbf{T}_i \delta \mathbf{u}_i \end{aligned} \tag{6}$$

Since nodal elastic virtual displacements ($\delta\mathbf{u}$) and nodal virtual displacements of the ERLS ($\delta\mathbf{r}$) are independent from each other, from the relations reported above the resulting equation describing the motion of the system is:

$$\begin{bmatrix} \mathbf{M} & \mathbf{MS} \\ \mathbf{S}^T\mathbf{M} & \mathbf{S}^T\mathbf{MS} \end{bmatrix} \begin{bmatrix} \ddot{\mathbf{u}} \\ \ddot{\mathbf{q}} \end{bmatrix} = \begin{bmatrix} \mathbf{f} \\ \mathbf{S}^T\mathbf{f} \end{bmatrix} \tag{7}$$

$\mathbf{M}$ is the mass matrix of the whole system and $\mathbf{S}$ is the sensitivity matrix for all the nodes. Isoparametric elements are used here, as in [38]. Vector $\mathbf{f} = \mathbf{f}(\mathbf{u}, \dot{\mathbf{u}}, \mathbf{q}, \dot{\mathbf{q}})$ takes account of all the forces affecting the system, including the gravity force. Adding a Rayleigh damping, right-hand side of Eq. (7) becomes:

$$\begin{bmatrix} \mathbf{f} \\ \mathbf{S}^T \end{bmatrix} = \begin{bmatrix} -2\mathbf{M}_G - \alpha\mathbf{M} - \beta\mathbf{K} & -\mathbf{M}\dot{\mathbf{S}} & -\mathbf{K} \\ \mathbf{S}^T(-2\mathbf{M}_G - \alpha\mathbf{M}) & -\mathbf{S}^T\mathbf{M}\dot{\mathbf{S}} & 0 \end{bmatrix} \begin{bmatrix} \dot{\mathbf{u}} \\ \dot{\mathbf{q}} \\ \mathbf{u} \end{bmatrix} + \begin{bmatrix} \mathbf{M} & \mathbf{I} \\ \mathbf{S}^T\mathbf{M} & \mathbf{S}^T \end{bmatrix} \begin{bmatrix} \mathbf{g} \\ \mathbf{F} \end{bmatrix} \tag{8}$$

P. Boscariol, A. Gasparetto
Model-based trajectory planning for flexible-link mechanisms with bounded jerk
Robotics and Computer Integrated Manufacturing 29(4), pp.90-99, 2013

Matrix $\mathbf{M}_G$ accounts for the Coriolis contribution, while $\mathbf{K}$ is the stiffness matrix of the whole system. α and β are the two Rayleigh damping coefficients. The system in eq. (7) can be made solvable by forcing to zero as many elastic displacement as the generalized coordinates, in this way ERLS position is defined univocally. So removing the displacement forced to zero from eq. (7) gives:

$$\begin{bmatrix} \mathbf{M}_{in} & (\mathbf{MS})_{in} \\ (\mathbf{S}^T\mathbf{M})_{in} & \mathbf{S}^T\mathbf{MS} \end{bmatrix} \begin{bmatrix} \ddot{\mathbf{u}}_{in} \\ \ddot{\mathbf{q}} \end{bmatrix} = \begin{bmatrix} \mathbf{f}_{in} \\ \mathbf{S}^T\mathbf{f} \end{bmatrix} \tag{9}$$

In this way, the values of the accelerations can be computed at each step by solving the system in (9), while the values of velocities and of displacements can be obtained by an appropriate integration scheme (e.g. the Runge-Kutta algorithm). It is important to focus the attention on the size and the rank of the matrices involved, and also to the choice of the general coordinates used in the ERLS definition. Otherwise it might happen that a singular configuration is encountered during the motion of the mechanism. In this case eq. (9) cannot be solved.

In order to define correctly the minimization problem that is used to evaluate an optimal motion profile, the direct dynamics of the flexible-link manipulator under consideration must be computed in its symbolic form. The reason of this need will be explained in the following section. Equation (9) can be rewritten by making explicit the state vector $\mathbf{x} = [\dot{\mathbf{u}}, \dot{\mathbf{q}}, \mathbf{u}, \mathbf{q}]^T$ and its time derivative, i.e. reducing the order of the ODE system in (9):

$$\begin{bmatrix} \mathbf{M} & \mathbf{MS} & 0 & 0 \\ \mathbf{S}^T\mathbf{M} & \mathbf{S}^T\mathbf{MS} & 0 & 0 \\ 0 & 0 & \mathbf{I} & 0 \\ 0 & 0 & 0 & \mathbf{I} \end{bmatrix} \begin{bmatrix} \ddot{\mathbf{u}} \\ \ddot{\mathbf{q}} \\ \dot{\mathbf{u}} \\ \dot{\mathbf{q}} \end{bmatrix} = \begin{bmatrix} \mathbf{M} & \mathbf{I} \\ \mathbf{S}^T\mathbf{M} & \mathbf{S}^T \\ 0 & 0 \\ 0 & 0 \end{bmatrix} \begin{bmatrix} \mathbf{g} \\ \mathbf{F} \end{bmatrix}$$
$$+ \begin{bmatrix} -2\mathbf{M}_G - \alpha\mathbf{M} - \beta\mathbf{K} & -\mathbf{M}\dot{\mathbf{S}} & -\mathbf{K} & 0 \\ -\mathbf{S}^T(2\mathbf{M}_G + \alpha\mathbf{M}) & -\mathbf{S}^T\mathbf{M}\dot{\mathbf{S}} & 0 & 0 \\ \mathbf{I} & 0 & 0 & 0 \\ 0 & \mathbf{I} & 0 & 0 \end{bmatrix} \begin{bmatrix} \dot{\mathbf{u}} \\ \dot{\mathbf{q}} \\ \mathbf{u} \\ \mathbf{q} \end{bmatrix} \tag{10}$$

or, in a more compact form:

$$\tilde{\mathbf{M}}\dot{\mathbf{x}} = \Phi(\mathbf{x}, \mathbf{F}, \mathbf{t}) \tag{11}$$

where:

$$\tilde{\mathbf{M}}(\mathbf{x}, t) = \begin{bmatrix} \mathbf{M} & \mathbf{MS} & 0 & 0 \\ \mathbf{S}^T\mathbf{MS} & \mathbf{S}^T\mathbf{MS} & 0 & 0 \\ 0 & 0 & \mathbf{I} & 0 \\ 0 & 0 & 0 & \mathbf{I} \end{bmatrix}$$

and

$$\mathbf{\Phi}(\mathbf{x}, \mathbf{F}, t) = \begin{bmatrix} \mathbf{M} & \mathbf{I} \\ \mathbf{S}^T\mathbf{M} & \mathbf{S}^T \\ 0 & 0 \\ 0 & 0 \end{bmatrix} \begin{bmatrix} \mathbf{g} \\ \mathbf{F} \end{bmatrix} + \begin{bmatrix} -2\mathbf{M}_G - \alpha\mathbf{M} - \beta\mathbf{K} & -\mathbf{M}\dot{\mathbf{S}} & -\mathbf{K} & 0 \\ \mathbf{S}^T(-2\mathbf{M}_G - \alpha\mathbf{M}) & -\mathbf{S}^\mathbf{T}\mathbf{M}\dot{\mathbf{S}} & 0 & 0 \\ \mathbf{I} & 0 & 0 & 0 \\ 0 & \mathbf{I} & 0 & 0 \end{bmatrix} \mathbf{x}$$

The direct dynamics of the manipulator is the first order ODE system:

$$\dot{\mathbf{x}} = \tilde{\mathbf{M}}(\mathbf{x}, t)^{-1} \Phi(\mathbf{x}, \mathbf{F}, t) \tag{12}$$

P. Boscariol, A. Gasparetto
Model-based trajectory planning for flexible-link mechanisms with bounded jerk
Robotics and Computer Integrated Manufacturing 29(4), pp.90-99, 2013

which must be computed in its symbolic explicit form. In order to do this, a symbolic algebraic tool must be used. In this case all the computation has been done using Matlab Symbolic Toolbox. The mechanism under consideration in this paper is not affected by gravity, therfore the gravitational term $\mathbf{g}$ in equation (10) is null. Moreover, if only rotary actuators are used, the vector of generalized forces $\mathbf{F}$ includes only torques and null terms. If τ_i is the torque produced by the i-th actuator and τ is the vector containing all the τ_i, $\mathbf{F}$ is simply $\mathbf{F} = \mathbf{F}(\tau)$. Therefore equation (12) can be rewritten as:

$$\dot{\mathbf{x}} = \tilde{\mathbf{M}}(\mathbf{x}, t)^{-1} \Phi(\mathbf{x}, \tau, t) = \Omega(\mathbf{x}, \tau, t) \tag{13}$$

Equation (13) can be rearranged to explicitely take into account the motor jerk γ, defined as the time derivative of the motor torque: $\gamma = \dot{\tau}$. A new augmented state vector can be defined as:

$$\mathbf{x}' = \begin{bmatrix} \mathbf{x} \\ \tau \end{bmatrix} \tag{14}$$

therefore a new formuation of eq. (13) can be written by a simple algebraic manipulation as:

$$\dot{\mathbf{x}'} = \mathbf{M}'(\mathbf{x}', t)^{-1} \Phi'(\mathbf{x}', \gamma, t) = \Omega'(\mathbf{x}', \gamma, t) \tag{15}$$

in which the explicit dependance of Φ' by torque τ is hidden and its role as the input variable has been taken by the actuator jerk γ.

3 Formulation of jerk-bounded motion planning problem

The target of this study is to find a way to compute a trajectory that brings the plant form a given initial condition $\mathbf{x}(t_0) = \mathbf{b}_0$ to the final configuration $\mathbf{x}(t_f) = \mathbf{b}_f$ in a given time. Among the infinite number of choices, the motion profile that we are looking for is the solution of the following optimization problem:

$$\begin{cases} \min\limits_{\gamma_i} J = \int\limits_{t_0}^{t_f} f(\mathbf{x}'(t), \gamma_i, t) dt + Z(\mathbf{x}'(t), \gamma_f, t_f) \\ subject\ to: \\ \dot{\mathbf{x}}'(t) = \Omega'(\mathbf{x}'(t), t, \gamma_i) \\ \Gamma^- \leq \gamma_i \leq \Gamma^+ \\ \mathbf{x}(t_0) = \mathbf{b}_0 \\ \mathbf{x}(t_f) = \mathbf{b}_f \end{cases} \tag{16}$$

f is a smooth differential function of the state variable $\mathbf{x}$ and of the control vector τ, while Z is a function of the system at terminal time, therefore is often referred as the terminal cost. Given the choice of the cost function J, the above problem is a Bolza problem. Since the problem is constrained by the nonlinear dynamic system $\Omega'(\mathbf{x}(t), t, \gamma_i)$ which represents the dynamics of the manipulator, the problem above is a nonlinear constrained optimization problem. One of the ways to solve it is to formulate a TPBVP (Two-Point Boundary Value Problem) trough the use of Pontryagin Minimum Principle (PMP) [39] and Hamilton-Jacobi-Bellman (HJB) equation. A good source of material on the calculus of variation and on the application of HJB equation and PMP can be found in the classic book [40]. A book more focused on practical applications is [41], which

P. Boscariol, A. Gasparetto
Model-based trajectory planning for flexible-link mechanisms with bounded jerk
Robotics and Computer Integrated Manufacturing 29(4), pp.90-99, 2013

covers also some basic numerical techniques often used for solving this class of problems.

The first step is to define the Hamiltonian, i.e. a function in the form:

$$\mathcal{H}(\mathbf{x}'(t), t, \gamma) = J + \Lambda^T \Omega'(\mathbf{x}'(t), t, \gamma) \tag{17}$$

where Λ is the vector of Lagrangian multipliers:

$$\Lambda = [\lambda_1, \lambda_2, \ldots, \lambda_n]^T$$

whose length is n, which equals the size of the state of the plant: $\mathbf{x}(t) \in \mathbb{R}^n$. Λ is also often called costate vector . Pontryagin Minimum Principle [39] states that the necessary conditions to obtain a solution to the problem stated in equation (16) are:

$$\dot{\mathbf{x}} = \frac{\partial \mathcal{H}}{\partial \Lambda} \tag{18}$$

$$\dot{\Lambda} = -\frac{\partial \mathcal{H}}{\partial \mathbf{x}} \tag{19}$$

$$0 = \frac{\partial \mathcal{H}}{\partial \gamma} \tag{20}$$

If constraints are present on the control vector γ, also the following must be taken into account:

$$\gamma = \begin{cases} \Gamma^+ & for \quad \gamma \geq \Gamma^+ \\ \gamma^* & for \quad \Gamma^- \leq \gamma \leq \Gamma^+ \\ \Gamma^- & for \quad \gamma \leq \Gamma^- \end{cases} \tag{21}$$

being γ^* the optimal control resulting from the equation (20). Among the infinite state trajectory that satisfy the conditions stated above, our goal is to choose the ones that respect the two boundary conditions at initial and final time t_0 and t_f. In general, such conditions can be posed on the so called augmented state, i.e. $\mathbf{y}(t) = [\mathbf{x}(t), \Lambda(t)]$, but in most cased such conditions are posed on the sole state vector of the plant $\mathbf{x}(t)$, since they have a straightforward physical meaning.

4 Reference mechanism

The mechanism taken as the testbench is a two-link planar RR manipulator with thin and long links. Actuation is provided by two torque controlled motors. The kinematic and dynamic characteristics of the manipulator are reported in Table 1. Link weight and flexural inertia are evaluated by choosing alluminum as the material of the links. Each link has a square section 1 cm wide, and the length of both links is 50 cm. Therefore the mass of each link is around 130 g. The weight of actuators and of end-effector tool are included by using concentrated masses at the nodes of the mechanism.

Each flexible link has been represented by a single finite element, using 6 d.o.f. Euler-Bernoulli elements. The rigid displacements q_1 and q_2 and the six elastic displacements u_1, u_2 ... u_6 are shown in Figure 2.

P. Boscariol, A. Gasparetto
Model-based trajectory planning for flexible-link mechanisms with bounded jerk
Robotics and Computer Integrated Manufacturing 29(4), pp.90-99, 2013

	symbol	value
Young's modulus	E	70×10^9 Pa
Flexural inertia moment	J	8.333×10^{-10} m^4
Beam width and thickness	a	10 mm
Length of first link	L_1	0.5 m
Length of second link	L_2	0.5 m
Mass/unit of length of links	m	0.27 kg/m
Concentrated mass at second joint	m_1	0.54 kg
Concentrared mass at the end-effector	m_2	0.2 kg
Rayleigh damping constants	α	7×10^{-2} s^{-1}
	β	2.1×10^{-5} s

Table 1: Kinematic and dynamic characteristics of the manipulator

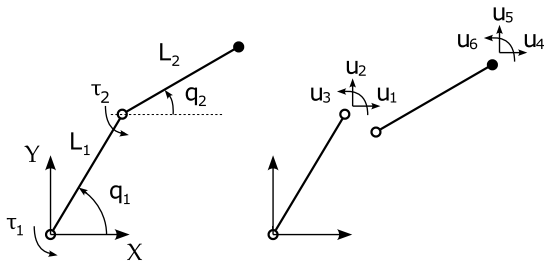

Figure 2: Two link manipulator: rigid and elastic displacements

5 Numerical results

The TPBVP problem stated in eq. (16) can be efficiently solved using the collocation method [41] Matlab routine "bvp4c" has proved to be quite efficient for the task, therefore it has been used to obtain all the results presented in this work. The formulation of the problem requires some symbolical computations that will be briefly summirized here. First of all, an explicit form of the direct dynamics of the manipulator must be available as a vector with 18 rows:

$$\Omega'(\mathbf{x}'(t), \gamma, t) \tag{22}$$

and the augmented state vector:

$$\mathbf{x}'(t) = [\dot{u}_1, \dot{u}_2, \ldots, \dot{u}_6, \dot{q}_1, \dot{q}_2, u_1, u_2, \ldots, u_6, q_1, q_2, \tau_1, \tau_2]^T \tag{23}$$

The control vector is $\mathbf{u} = [\gamma_1, \gamma_2]^T$. The cost function of choice is:

$$f = \mathbf{u}^T \mathbf{R} \mathbf{u} + \mathbf{x'}^T \mathbf{Q} \mathbf{x'} \tag{24}$$

where $\mathbf{R}$ is a 2×2 matrix that weigth the value of the control input (i.e. the actuator jerks), while $\mathbf{Q}$ is a 18×18 matrix that penalizes the various entries of the augmented state vector $\mathbf{x}'$. $\mathbf{R}$ and $\mathbf{Q}$ have been chosen to be diagonal matrices: this choice makes the cost function J to be quadratic. The Hamiltonian already expressed in (17) can be evalued in its sybolic form once the costate vector is defined:

$$\Lambda = [\lambda_1, \lambda_2, \ldots, \lambda_{18}]^T \tag{25}$$

P. Boscariol, A. Gasparetto
Model-based trajectory planning for flexible-link mechanisms with bounded jerk
Robotics and Computer Integrated Manufacturing 29(4), pp.90-99, 2013

Λ has 18 entries, i.e. has the same size of the augmented state vector $\dot{\mathbf{x}}'$. Once the Hamiltonian is computed, the new ODE system can be computed:

$$\dot{\mathbf{y}} = \begin{bmatrix} \dfrac{\partial \mathcal{H}}{\partial \Lambda} \\ \\ -\dfrac{\partial \mathcal{H}}{\partial \mathbf{x}'} \end{bmatrix} \tag{26}$$

Then the optimal control can be computed using eq. (20) solving it for the motor jerks γ_1 and γ_2. The optimal controls are referred as: ${\gamma_1}^*$ and ${\gamma_2}^*$. Such expressions can be subtituted into (26) leading to:

$$\dot{\mathbf{y}}^* = \begin{bmatrix} \dfrac{\partial \mathcal{H}^*(\mathbf{x}', \Lambda, {\gamma_1}^*, {\gamma_2}^*)}{\partial \Lambda} \\ \\ -\dfrac{\partial \mathcal{H}^*(\mathbf{x}', \Lambda, {\gamma_1}^*, {\gamma_2}^*)}{\partial \mathbf{x}'} \end{bmatrix} \tag{27}$$

Now a suitable set of boundary values must be chosen to complete the definition of a Two-Point Boundary Value Problem. The numerical method used in this paper, i.e. the collocation method, require for the number of boundary conditions to be equal to the number of entries of the ODE system in eq. (27), which is 36. Therefore we impose 18 bounday conditions on the state variables at $t = 0$ and 18 boundary conditions at final time $t = t_f$. All the bounday conditions are null, with the exception of the initial and final rigid displacments q_1 and q_2. In this way we obtain a rest-to-rest motion with null initial and final displacements, and moreover also their time derivative will be equal to zero, as well as null velocity at the joints. The values of $q_1(0)$, $q_2(0)$, $q_1(t_f)$ and $q_2(t_f)$ have been computed using a kinematic inversion algorithm from the intial and final positions of the end-effector. For all the test reported in this section, the initial and final position of the end effector measured in the X, Y plane are $(0, -1)$ and $(0, 0.5)$, respectively. In this way a large displacement of the two links is performed in 1 second.

5.1 Minimum jerk problem

The first test case involves the planning of a minimum jerk trajectory. Therefore the cost function of choice is:

$$J = \int_{t_0}^{t_f} \gamma^T \mathbf{R} \gamma dt \tag{28}$$

being $\gamma = [\gamma_1, \gamma_2]^T$ the vector of motor jerk, and $\mathbf{R}$ a diagonal matrix of weights. In this way the optimization procedure produces a trajectory with minimum integral of the quadratic norm of the jerk along the whole trajectory. Moreover the resulting trajectory is smooth, meaning that there are no discontinuities in the jerk profiles. Literature on trajectory planning has in many cases highlighted the worsening on motion accuracy and the increased level of vibration on the end effector caused by high level of acceleration and jerk as in [42, 43, 44, 45]. In particular Zefran et. al. in [46] shows that smooth trajectories (i.e. trajectories without jerk discontinuities) are to be preferred to comply with the physical limitation of the actuators and with the limits of the control system bandwidth, and that non-smooth motion can excite the structural natural frequencies of the

P. Boscariol, A. Gasparetto
Model-based trajectory planning for flexible-link mechanisms with bounded jerk
Robotics and Computer Integrated Manufacturing 29(4), pp.90-99, 2013

system. Another example that uses minimum integral of jerk for planning smooth trajectories is [47]. All the results presented in Figures (3-10) refer to the case in which $\mathbf{R} = \begin{bmatrix} 1 & 0 \\ 0 & 1 \end{bmatrix}$. Figure 3 shows the trajectory of the end-effector during the motion. The end-effector of the manipulator moves form point A to point B. The position of each link is showed every 50 ms. Motor toques and jerk are shown in Figure (4) and (5), respectively. The anlysis of such data shows that the torque profiles are very smooth, and that the jerk values, while being quite high at the start and end point, are continuous. The angular position of the links, measured in the global reference frame X, Y somehow resemble two sigmoid functions, as it can be seen in Figure (6). In order to evaluate the level of vibration induced on the structure of the manipulator, the time evolution of the two link curvatures are reported in Figures (7 8) for clarity, instead of showing the nodal displacements, which have a less straightforward physical interpretation. Taking into consideration the *i*-th link of the kinematic chain, its curvature can be calculated as:

$$C_i = \mathbf{H}_i \mathbf{u}_i \tag{29}$$

being $\mathbf{u}_i$ the vector of 6 nodal displacements, and $\mathbf{H}_i$ a matrix of coefficients evaluated as:

$$\mathbf{H}_i = \mathbf{B}_i(x_i, y_i)\mathbf{T}_i(q_i) \tag{30}$$

$\mathbf{T}_i(q)$ is the global-to-local transformation matrix already introduced in (5), while $\mathbf{B}_i(x_i, y_i)$ is the strain-displacement matrix also introduced in eq. (6). x_i and y_i are the coordinates of the local reference frame at which the curvature is calculated. Another reason for the use of curvature, is that it can be directly measured using a strain gauge bridge. Analysis of Figures (7,8) shows that the elastic displacement of the link is quite limited, considered the high flexibility of the structure and the speed of motion achieved. A more detailed information can be obtained trough the spectral analysis of this signals. Figures 9 and 10, which plots the Fast Fourier Transform (FFT) of the curvature signal, shows that the principal vibration components, located at 67 Hz for the first link and at 66 Hz for the second link, have a low peak amplitude, i.e. -76.89 dB and -78.19 dB respectively. Higher frequency modes have and even smaller amplitudes, being lower than 100 dB. As it will be shown in the following section, this good results can be even improved by using a more sophisticated cost funcion an by including jerk constraints in the otpimization problem.

5.2 Composite cost function problem with constrained jerk

The second test case takes into consideration the same manipulator and the same task used for the previous results. The difference here is that the cost function J is now composite, since it takes into consideration also weights on motor torques, on nodal displacements, on their time derivative, on rigid displacments and on joint speed. Therefore the problem in equation (16) uses the following cost function J:

$$J = \int_{t_0}^{t_f} \left(\gamma^T \mathbf{R} \gamma + \tau^T \mathbf{Q}_\tau \tau + \mathbf{u}^T \mathbf{Q}_u \mathbf{u} + \dot{\mathbf{u}}^T \mathbf{Q}_{\dot{u}} \dot{\mathbf{u}} + \mathbf{q}^T \mathbf{Q}_q \mathbf{q} + \dot{\mathbf{q}}^T \mathbf{Q}_{\dot{q}} \dot{\mathbf{q}} \right) dt \tag{31}$$

Since all the weigthing matrices in equation (31) are diagonal, the optimization problem is stilll quadratic. The complexity of the cost function allows to

P. Boscariol, A. Gasparetto
Model-based trajectory planning for flexible-link mechanisms with bounded jerk
Robotics and Computer Integrated Manufacturing 29(4), pp.90-99, 2013

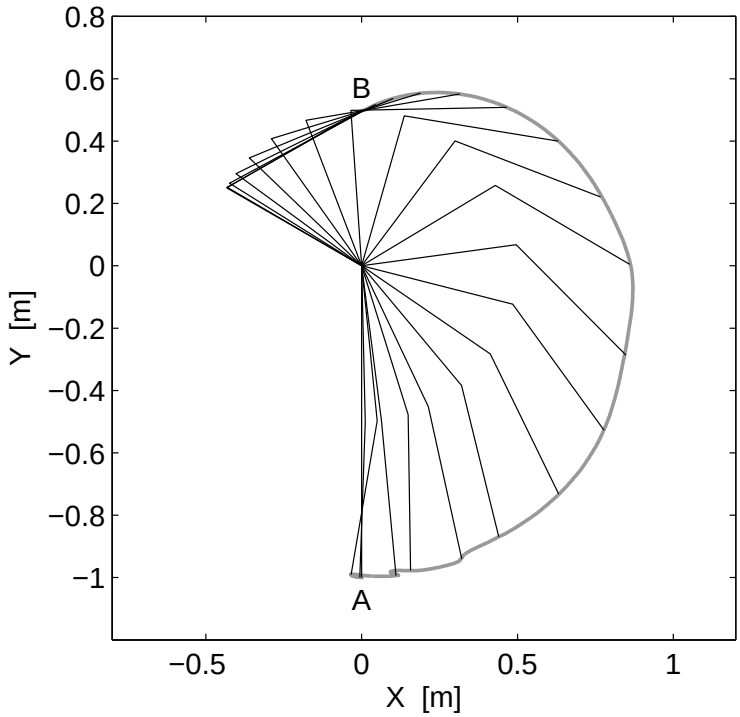

Figure 3: Trajectory of the end-effector in the operative space: min jerk solution

precisely tailor the resulting trajectory. Each weighting matrix allows to penalize large values of all the components of the state variable $\mathbf{x}'$: matrix $\mathbf{Q}_q$ keeps undel control large variations of the angular position of the links. Similar effects on elastic deformations, joint speeds and torques are induced by setting high values on $\mathbf{Q}_u$, $\mathbf{Q}_{\dot{q}}$ and $\mathbf{Q}_\tau$ respectively. Of particular interest is the use of the weighting matrix $\mathbf{Q}_{\dot{\mathbf{u}}}$: its role is to penalize the drivative of the nodal elastic displacement, i.e. it can significantly reduce the high-order harmonic content of elastic deformations. The results presented in this section include both an unconstrained and a constrained problem. For the latter, the motor jerk is limited to the range ± 10 Nm/s. The weighting matrices used for the two tests cases presented here are:

$$\mathbf{R} = \begin{bmatrix} 5 & 0 \\ 0 & 5 \end{bmatrix} \quad \mathbf{Q}_\tau = \begin{bmatrix} 1 & 0 \\ 0 & 1 \end{bmatrix} \quad \mathbf{Q}_q = \begin{bmatrix} 1 & 0 \\ 0 & 1 \end{bmatrix} \quad \mathbf{Q}_{\dot{q}} = \begin{bmatrix} 5 & 0 \\ 0 & 5 \end{bmatrix}$$

$$\mathbf{Q}_u = \begin{bmatrix} 5 & 0 & 0 & 0 & 0 & 0 \\ 0 & 5 & 0 & 0 & 0 & 0 \\ 0 & 0 & 5 & 0 & 0 & 0 \\ 0 & 0 & 0 & 5 & 0 & 0 \\ 0 & 0 & 0 & 0 & 5 & 0 \\ 0 & 0 & 0 & 0 & 0 & 5 \end{bmatrix} \quad \mathbf{Q}_{\dot{u}} = \begin{bmatrix} 12 & 0 & 0 & 0 & 0 & 0 \\ 0 & 12 & 0 & 0 & 0 & 0 \\ 0 & 0 & 12 & 0 & 0 & 0 \\ 0 & 0 & 0 & 12 & 0 & 0 \\ 0 & 0 & 0 & 0 & 12 & 0 \\ 0 & 0 & 0 & 0 & 0 & 12 \end{bmatrix}$$

Figure 11 shows the trajectory of the end-effector, while Figure 14 shows the evolutions of the two angular positions, including both the constrained and unconstrained solutions. A simple analysis of the two figures shows that the two trajectory are quite similar, but the unconstrained solution has a slight oscillation on the q_2 profile which is less prominent in the constrained jerk case. Angular

P. Boscariol, A. Gasparetto
Model-based trajectory planning for flexible-link mechanisms with bounded jerk
Robotics and Computer Integrated Manufacturing 29(4), pp.90-99, 2013

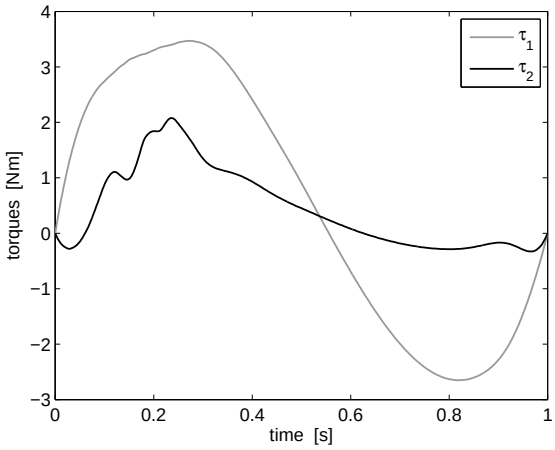

Figure 4: Motor torques: min jerk solution

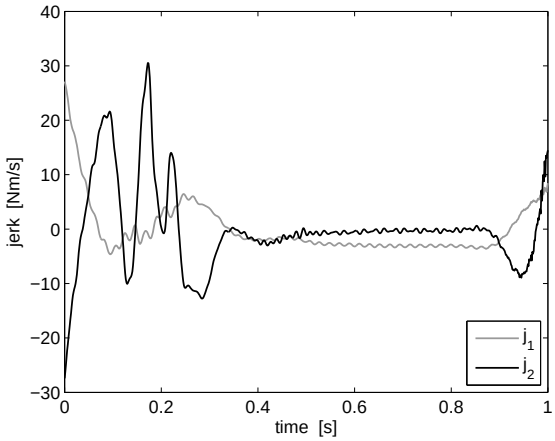

Figure 5: Jerk profiles: min jerk solution. j_1 and j_2 are the jerk for the first and second joint

position q_1 is actually not influenced by the jerk constraint. Motor torques are displayed in Figure 12: here it is evident that the torque profiles are again similar in the constrained and unconstrained cases, but the introduction of the constraint on jerk has the influence of increasing the peak value of torque τ_1. Jerk profiles are displayed in Figure 13: here it can be seen that the unconstrained solution has torques as high as 27 and 50 Nm/s for the first and second motor, respectively, while the constrained solution limits them in the $\pm 10\ Nm/s$ range. The limitation happens mostly during the intial and final phases of motion, i.e. the most criticial phases for the development of a damped response. Elastic displacements are shown in Figure (15 and 16) as link curvatures. Here it is visible that the use of jerk constraints improves by a large amount the amplitude of vibration, whose peak values are roughly halved for both links. The frequency spectrum of these signals are displayed in Figures (17, 18): from the analysis of plots it can be ssen that there is a reduction in the peak value located around 67 Hz for both links of roughly 10 dB. A comparison of the peak amplitudes of the frequency spectrum of link curvatures is reported in Table 3. This modal component is the only actually

P. Boscariol, A. Gasparetto
Model-based trajectory planning for flexible-link mechanisms with bounded jerk
Robotics and Computer Integrated Manufacturing 29(4), pp.90-99, 2013

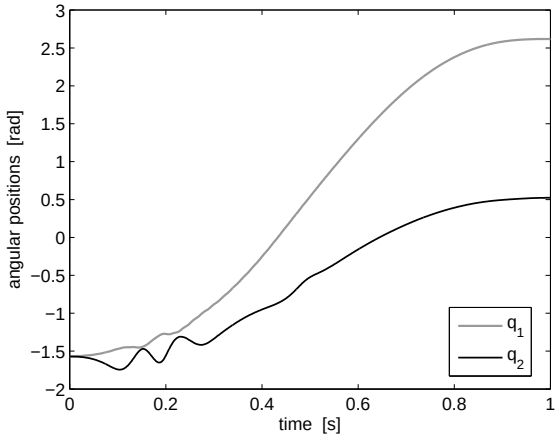

Figure 6: Joint position profiles: min jerk solution. q_1 and q_2 are the angualr positions of the first and second joint, respectively

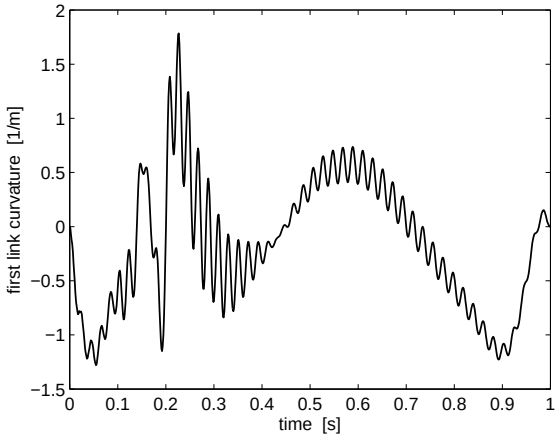

Figure 7: Curvature at the mdispan of the fisrt link: min jerk solution

significant one in the frequency spectrum, meaning that higher oder modes are basically not excited by the motion profile.

Peak value of jerk and torque for the three test cases developed in this work are shown in table 2.

P. Boscariol, A. Gasparetto
Model-based trajectory planning for flexible-link mechanisms with bounded jerk
Robotics and Computer Integrated Manufacturing 29(4), pp.90-99, 2013

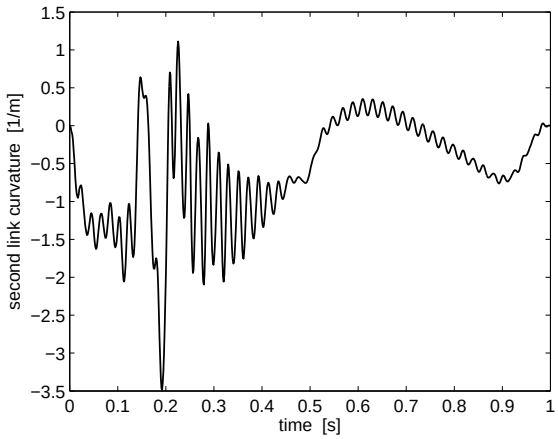

Figure 8: Curvature at the mdispan of the second link: min jerk solution

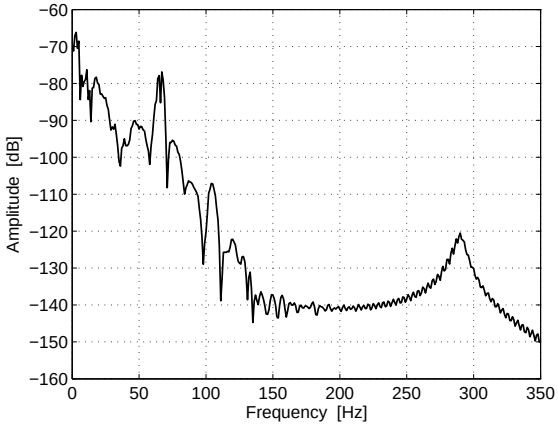

Figure 9: Frequency spectrum of the curvature the mdispan of the first link: min jerk solution

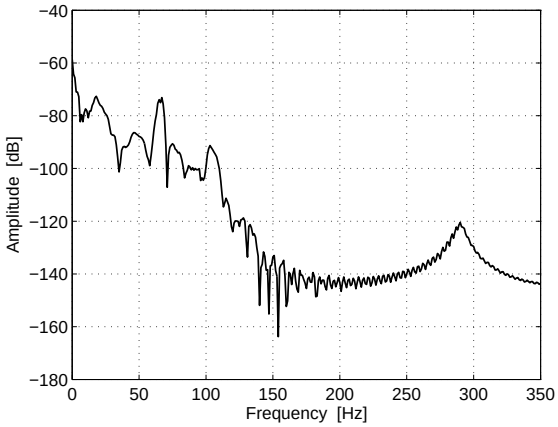

Figure 10: Frequency spectrum of the curvature the mdispan of the second link: min jerk solution

P. Boscariol, A. Gasparetto
Model-based trajectory planning for flexible-link mechanisms with bounded jerk
Robotics and Computer Integrated Manufacturing 29(4), pp.90-99, 2013

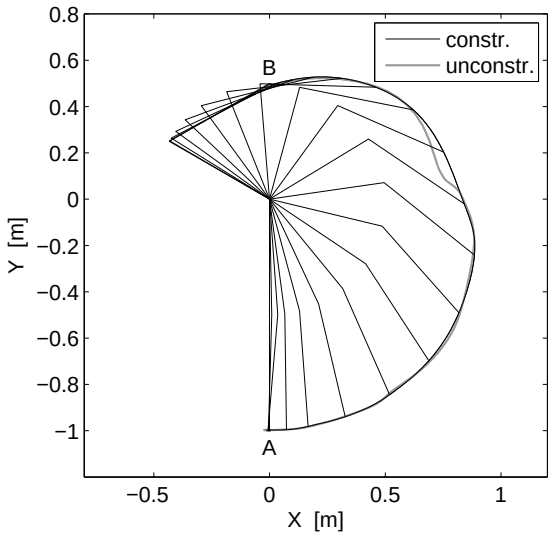

Figure 11: Trajectory of the end-effector in the operative space: constrained and unconstrained (*) solutions

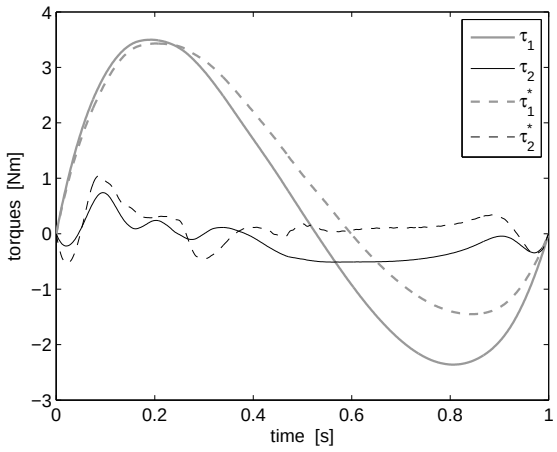

Figure 12: Motor torques: constrained and unconstrained (*) solution

peak torque [Nm]	MJ	CCF	CONSTR
τ_1	3.431	3.429	3.498
τ_2	1.04	0.7412	1.04
peak jerk $[Nm/s]$	MJ	CCF	CONSTR
j_1	55.76	55.76	10
j_2	27.35	27.35	10

Table 2: Comparison of results: min jerk (MJ) solution, composite cost function (CCF), constrained jerk solution (CONSTR)

P. Boscariol, A. Gasparetto
Model-based trajectory planning for flexible-link mechanisms with bounded jerk
Robotics and Computer Integrated Manufacturing 29(4), pp.90-99, 2013

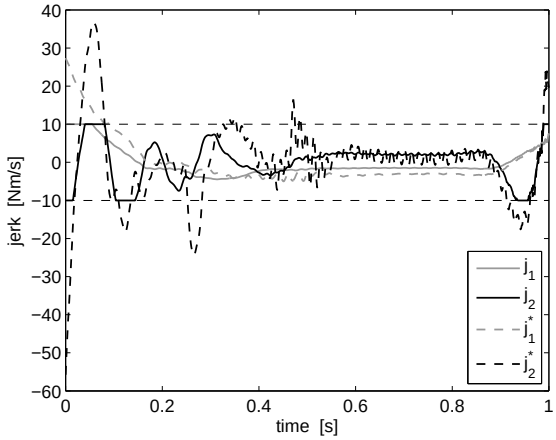

Figure 13: Jerk profiles: constrained and unconstrained (*). j_1 and j_2 are the jerks for the first and second joint, respectively

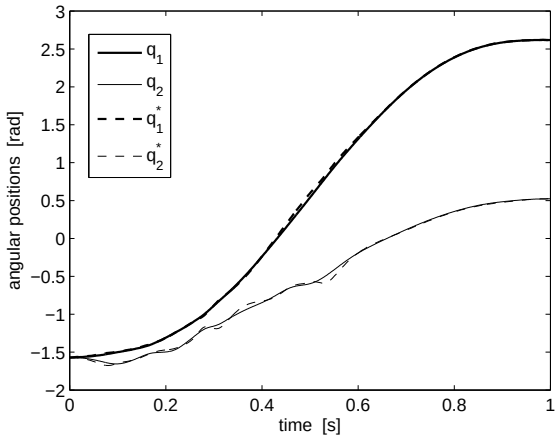

Figure 14: Joint position profiles: constrained and unconstrained (*) solution. q_1 and q_2 are the angular position of the first and second joint,respectively

First link			
MJ	CCF	CONSTR	Frequency
-76.80	-80.88	-90.8	67 Hz
-107.2	-115	-125	105 Hz
-116.8	-116.8	-122.9	290 Hz
Second link			
MJ	CCF	CONSTR	Frequency
-78.319	-78.19	-88.78	66 Hz
-91.26	-91.26	-113.5	97 Hz
-116.8	-116.8	-122.8	290 Hz

Table 3: Comparison of results as peak values of spectral components of link curvature [dB]: min jerk (MJ) solution, composite cost function (CCF), constrained jerk solution (CONSTR)

P. Boscariol, A. Gasparetto
Model-based trajectory planning for flexible-link mechanisms with bounded jerk
Robotics and Computer Integrated Manufacturing 29(4), pp.90-99, 2013

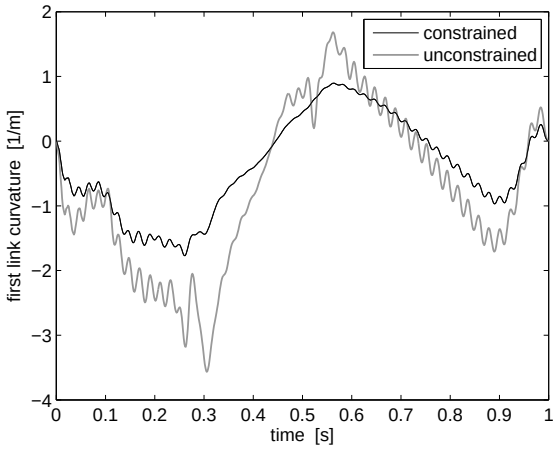

Figure 15: Curvature at the mdispan of the fisrt link: constrained and unconstrained solution

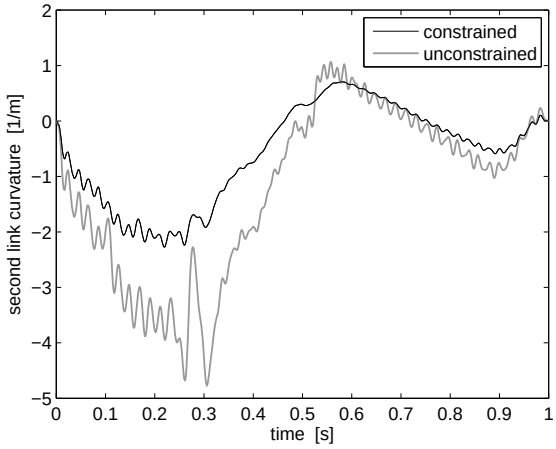

Figure 16: Curvature at the mdispan of the second link: constrained and unconstrained solution

P. Boscariol, A. Gasparetto
Model-based trajectory planning for flexible-link mechanisms with bounded jerk
Robotics and Computer Integrated Manufacturing 29(4), pp.90-99, 2013

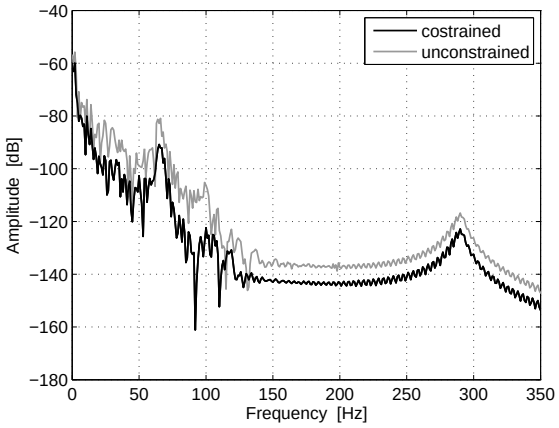

Figure 17: Frequency spectrum of the curvature the mdispan of the first link: constrained and unconstrained solution

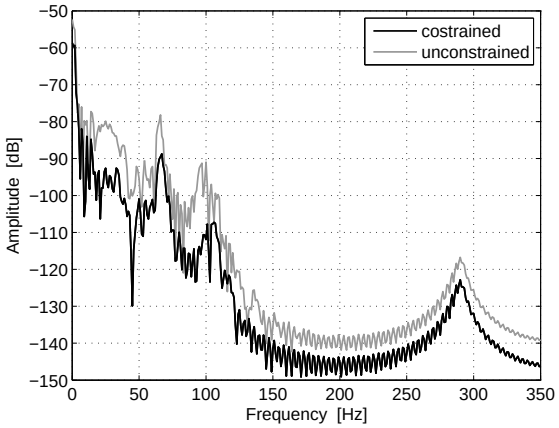

Figure 18: Frequency spectrum of the curvature the mdispan of the second link: constrained and unconstrained solution

6 Conclusion

In this paper the problem of planning of jerk-constrained trajectory for flexible-links mechanisms has been investigated. Unlike most of the available literature on the subject, dynamic modelling of FLMs is achieved trough the use of a nonlineare FEM-based approach, for maximum accuracy. The optimization problem is set as a nonlinear constrained optimization problem, which is translated into a two-point boundary value problem and solved numerically. Jerk optimal and composite cost optimal with bounded jerk solution are achieved by a redefinition of the ODE system that represents the dynamics of the system. The capability of the proposed approach is tested here, by showing that the use of constraints on the computation of jerk profiles and the use of a complex composite function can lead to the determination of trajectories with very limited vibrational phenomena. The testbench is an RR mechanisms (i.e. a robot with two revolute joints) with flexible links. The frequency analysis of the displacement measurements shows that the jerk limitation can achieve vibration reductions in the order of 10 dB for the main modal components, and that the magnitued of higher-order modes are basically not excited by the motion profiles.

References

[1] S. Dwivedy, P. Eberhard, Dynamic analysis of flexible manipulators, a literature review, Mechanism and Machine Theory 41 (7) (2006) 749–777.

[2] R. D. Robinett, D. G. Wilson, G. R. Eisler, J. E. Hurtado, Applied dynamic programming for optimization of dynamical systems (Advances in design and control), SIAM - Society for Industrial and Applied Mathematics, Philadelphia, 2005, pp. 151–170.

[3] R. Theodore, A. Ghosal, Comparison of the assumed modes and finite element models for flexible multi-link manipulators, The International journal of robotics research 14 (2) (1995) 91–111.

[4] W. Chen, Dynamic modeling of multi-link flexible robotic manipulators, Computers & Structures 79 (2) (2001) 183–195.

[5] R. Milford, S. Asokanthan, Configuration dependent eigenfrequencies for a two-link flexible manipulator: Experimental verification, Journal of sound and vibration 222 (2) (1999) 191–207.

[6] D. Turcic, A. Midha, J. Bosnik, Dynamic analysis of elastic mechanism systems. ii: Experimental results, Journal of dynamic systems, measurement, and control 106 (4) (1984) 255–260.

[7] C. Damaren, I. Sharf, Simulation of flexible-link manipulators with inertial and geometric nonlinearities, Journal of dynamic systems, measurement, and control 117 (1) (1995) 74–87.

[8] A. De Luca, B. Siciliano, Closed-form dynamic model of planar multilink lightweight robots, IEEE Transactions on Systems, Man and Cybernetics 21 (4) (1991) 826–839.

[9] S. Tadikonda, H. Baruh, Dynamics and control of a translating flexible beam with a prismatic joint, Journal of dynamic systems, measurement, and control 114 (1992) 422–427.

[10] H. Lee, New dynamic modeling of flexible-link robots, Journal of dynamic systems, measurement, and control 127 (2) (2005) 307–309.

[11] M. Giovagnoni, A numerical and experimental analysis of a chain of flexible bodies, Journal of dynamic systems, measurement, and control 116 (1) (1994) 73–80.

[12] A. Gasparetto, V. Zanotto, A new method for smooth trajectory planning of robot manipulators, Mechanism and Machine Theory 42 (4) (2007) 455–471.

[13] O. von Stryk, M. Schlemmer, Optimal control of the industrial robot manutec r3, in: Computational optimal control, Birkhauser Verlag, Basel, 1994, pp. 367–382.

[14] T. Chettibi, P. Lemoine, Generation of point to point trajectories for robotic manipulators under electro-mechanical constraints, International Review of Mechanical Engineering (I.RE.M.E.) 1 (2) (2007) 131–143.

[15] H. Xu, J. Zhuang, S. Wang, Z. Zhu, Global time-energy optimal planning of robot trajectories, in: International Conference on Mechatronics and Automation (ICMA), IEEE, 2009, pp. 4034–4039.

[16] H. Liu, X. Lai, S. Zhu, X. Liao, Jerk-bounded and -continuous trajectory planning for a 6-dof serial robot manipulator with revolute joints, in: 30th Chinese Control Conference (CCC), IEEE, 2011, pp. 3462–3466.

[17] M. Ghasemi, N. Kashiri, M. Dardel, Time-optimal trajectory planning of robot manipulators in point-to-point motion using an indirect method, Proceedings of the Institution of Mechanical Engineers, Part C: Journal of Mechanical Engineering Science 226 (2) (2012) 473–484.

[18] D. Balkcom, M. Mason, Time optimal trajectories for bounded velocity differential drive vehicles, The International Journal of Robotics Research 21 (3) (2002) 199–217.

[19] O. Dahl, Path constrained motion optimization for rigid and flexible joint robots, in: International Conference on Robotics and Automation, Vol. 2, IEEE, 1993, pp. 223–229.

[20] M. Korayem, H. R. Nohooji, A. Nikoobin, Optimal motion generating of nonholonomic manipulators with elastic revolute joints in generalized point-to-point task, International journal of advanced design and manufacturing technology 3 (2) (2010) 1–9.

[21] G. Boschetti, D. Richiedei, A. Trevisani, Delayed reference control for multi-degree-of-freedom elastic systems: Theory and experimentation, Control Engineering Practice 19 (9) (2011) 1044–1055.

[22] G. Boschetti, D. Richiedei, A. Trevisani, Delayed reference control applied to flexible link mechanisms: A scheme for effective and stable control, Journal of dynamic systems, measurement, and control 134 (1).

[23] A. Abe, Trajectory planning for residual vibration suppression of a two-link rigid-flexible manipulator considering large deformation, Mechanism and machine theory 44 (9) (2009) 1627–1639.

[24] D. Hull, Conversion of optimal control problems into parameter optimization problems, Journal of guidance, control, and dynamics 20 (1) (1997) 57–62.

[25] H. Kojima, T. Kibe, Optimal trajectory planning of a two-link flexible robot arm based on genetic algorithm for residual vibration reduction, in: IEEE/RSJ International Conference on Intelligent Robots and Systems, Vol. 4, 2001, pp. 2276–2281.

[26] K. J. Park, Flexible robot manipulator path design to reduce the endpoint residual vibration under torque constraints, Journal of Sound and Vibration 275 (3) (2004) 1051–1068.

[27] W. Faris, A. Ata, M. Sa'adeh, Energy minimization approach for a two-link flexible manipulator, Journal of Vibration and Control 15 (4) (2009) 497–526.

[28] K. J. Park, Modeling and control of a two-link flexible manipulator using fuzzy logic and genetic optimization techniques, Journal of Sound and Vibration 275 (3) (2004) 1051–1068.

[29] D. G. Wilson, R. D. Robinett, G. R. Eisler, Discrete dynamic programming for optimized path planning of flexible robots, in: IEEE/RSJ International Conference on Intelligent Robots and Systems, Vol. 3, Sendai, Japan, 2004, pp. 2918–2923.

[30] R. E. Bellman, Dynamic programming, Princeton University Press, Princeton, 1957.

[31] M. Korayem, A. Nikoobin, V. Azimirad, Trajectory optimization of flexible link manipulators in point-to-point motion, Robotica 27 (6) (2009) 825–840.

[32] D. Kirk, Optimal control theory: an introduction, Prentice-Hall, 1970.

[33] M. Korayem, M. Haghpanahi, H. Rahimi, A. Nikoobin, Finite element method and optimal control theory for path planning of elastic manipulators, New Advances in Intelligent Decision Technologies 199 (2009) 117–126.

[34] A. Gasparetto, On the modeling of flexible-link planar mechanisms: experimental validation of an accurate dynamic model, Journal of dynamic systems, measurement, and control 126 (2004) 365–375.

[35] R. Caracciolo, D. Richiedei, A. Trevisani, Experimental validation of a model-based robust controller for multi-body mechanisms with flexible links, Multibody System Dynamics 20 (2) (2008) 129–145.

[36] R. Caracciolo, D. Richiedei, A. Trevisani, Design and experimental validation of piecewise-linear state observers for flexible link mechanisms, Meccanica 41 (6) (2006) 623–637.

[37] L. Chang, K. Gannon, A dynamic model on a single-link flexible manipulator, Journal of Vibration and Acoustics 112 (1990) 138.

[38] M. Giovagnoni, Simplifications using isoparametric elements in flexible linkage analysis, International Journal for Numerical Methods in Engineering 28 (4) (1989) 967–977.

[39] L. Pontriagin, R. Gamkrelidze, The mathematical theory of optimal processes, Vol. 4, CRC, 1986.

[40] D. Kirk, Optimal control theory: an introduction, Dover Pubns, 2004.

[41] L. Shampine, I. Gladwell, S. Thompson, Solving ODEs with MATLAB, Cambridge University Press, 2003.

[42] P. Barre, R. Bearee, P. Borne, E. Dumetz, Influence of a jerk controlled movement law on the vibratory behaviour of high-dynamics systems, Journal of Intelligent & Robotic Systems 42 (3) (2005) 275–293.

[43] E. Dumetz, J. Dieulot, P. Barre, F. Colas, T. Delplace, Control of an industrial robot using acceleration feedback, Journal of Intelligent & Robotic Systems 46 (2) (2006) 111–128.

[44] A. Olabi, R. Béarée, O. Gibaru, M. Damak, Feedrate planning for machining with industrial six-axis robots, Control Engineering Practice 18 (5) (2010) 471–482.

[45] A. Gasparetto, P. Boscariol, A. Lanzutti, R. Vidoni, Trajectory planning in robotics, Mathematics in Computer Science (2012) 1–11.

[46] M. Zefran, V. Kumar, C. Croke, On the generation of smooth three-dimensional rigid body motions, Robotics and Automation - IEEE Transactions on 14 (4) (1998) 576–589.

[47] V. Zanotto, A. Gasparetto, A. Lanzutti, P. Boscariol, R. Vidoni, Experimental validation of minimum time-jerk algorithms for industrial robots, Journal of Intelligent & Robotic Systems 64 (2) (2011) 197–219.

P. Boscariol, A. Gasparetto
Model-based trajectory planning for flexible-link mechanisms with bounded jerk
Robotics and Computer Integrated Manufacturing 29(4), pp.90-99, 2013